Applied Physics Letters

Generation of an ultra-long sub-diffracted second-harmonic optical needle from a periodically poled $LiNbO_3$ crystal

Cite as: Appl. Phys. Lett. **116**, 081106 (2020); https://doi.org/10.1063/1.5142522
Submitted: 14 December 2019 . Accepted: 20 February 2020 . Published Online: 27 February 2020

Yunzhi Zhu, Huijun Wang, Yihong Zhang, Dongmei Liu, Weihao Zhong, Zhida Gao, Guoxin Cui, Yanqing Lu, Yong Zhang, and Min Xiao

Applied Physics Letters ARTICLE scitation.org/journal/apl

Generation of an ultra-long sub-diffracted second-harmonic optical needle from a periodically poled $LiNbO_3$ crystal

Cite as: Appl. Phys. Lett. **116**, 081106 (2020); doi: 10.1063/1.5142522
Submitted: 14 December 2019 · Accepted: 20 February 2020 ·
Published Online: 27 February 2020

Yunzhi Zhu,[1] Huijun Wang,[1] Yihong Zhang,[1] Dongmei Liu,[2,a)] Weihao Zhong,[1] Zhida Gao,[3] Guoxin Cui,[1] Yanqing Lu,[1] Yong Zhang,[1,b)] and Min Xiao[1,4]

AFFILIATIONS

[1]National Laboratory of Solid State Microstructures, College of Engineering and Applied Sciences, School of Physics, and Collaborative Innovation Center of Advanced Microstructures, Nanjing University, Nanjing 210093, China
[2]School of Physics and Telecommunication Engineering, South China Normal University, Guangzhou 510006, China
[3]College of Science, Northeastern University, 110004 Shenyang, China
[4]Department of Physics, University of Arkansas, Fayetteville, Arkansas 72701, USA

[a)]Email: dmliu@scnu.edu.cn
[b)]Author to whom correspondence should be addressed: zhangyong@nju.edu.cn

ABSTRACT

We experimentally demonstrate the use of a periodically poled $LiNbO_3$ (PPLN) crystal to produce an ultra-long sub-diffraction optical needle via second-harmonic generation. When we input a radially polarized fundamental wave from a femtosecond laser, a sub-diffraction beam size of $0.45\lambda_{SH}$ and an ultra-long depth of focus (DOF) of $55\lambda_{SH}$ are experimentally realized, where λ_{SH} is the second harmonic wavelength. The lateral size of the second harmonic optical needle is reduced by a factor of 2 compared to the case using the fundamental wave. The compact experimental configuration can realize wavelength conversion and wave-front shaping simultaneously in a single PPLN crystal. In addition, the ultra-long DOF is potentially useful in observing thick samples. The unique characteristics of our second harmonic optical needle open the door for practical applications in super-resolution imaging and optical manipulation.

Observation of sub-wavelength structures using a conventional optical imaging system such as a microscope, a telescope, or a camera used to be difficult because of the Abbe diffraction limit.[1] At the end of the 20th century, this theory was challenged and was disproven; several revolutionary breakthroughs were realized to overcome Abbe's diffraction limit, including stimulated emission depletion (STED) microscopy,[2,3] photoactivation localization microscopy (PALM),[4] stochastic optical reconstruction microscopy (STORM),[5] structured illumination microscopy (SIM),[6,7] and monomolecular spectroscopy.[8,9] Recently, optical needles with a sub-diffraction size have been attracting increased interest.[10–12] Optical needles can be achieved using super-oscillatory lenses,[13,14] binary elements,[11,15,16] or a meta-surface.[17,18] The generation of optical needles, to date, has been limited to linear optics.

Nonlinear optics has a wide range of important applications, including nonlinear conversion of orbital angular momentum,[19–21] ultrashort pulse generation,[22,23] quantum light sources,[24] and optical communications.[25] Large numbers of optical materials have been explored and applied in an attempt to achieve efficient nonlinear optical processes, including semiconductors,[26,27] metal oxides,[28] and polymers.[29] Among these materials, the $LiNbO_3$ crystal offers incredible versatility because of its broad transmission range from the visible to the mid-infrared range and high nonlinear coefficients. Specifically, based on quasi-phase matching (QPM) theory, periodically poled $LiNbO_3$ (PPLN) crystals have been extensively investigated in frequency conversion,[30,31] nonlinear waveguides,[32] and nonlinear beam shaping for the generations of second harmonic (SH) Airy beams, SH vortex beams, and so on.[33,34]

In this paper, we propose and experimentally demonstrate an SH optical needle using a PPLN crystal excited by a radially polarized light. Ring-shaped domain structures via the electrical poling process are introduced to realize a sub-diffraction optical needle. There is a π phase shift between the SH waves from opposite domain structures. In comparison to the linear optical method, the beam size of the SH optical needle is reduced by two times due to frequency doubling. The ring-shaped domain structure is used to work as a nonlinear frequency

converter.[35–37] In our experiment, such binary nonlinear phase modulation is capable of producing an optical needle with a sub-diffracted beam size of about $0.45\lambda_{SH}$ and an ultra-long depth of focus (DOF) of about $55\lambda_{SH}$ (where λ_{SH} is the second harmonic wavelength), which is much longer than that reported in previous works.[11–15,38]

To design an appropriate domain structure to generate a sub-diffraction optical needle, we investigate the electrical field distribution behind the PPLN sample theoretically. Noting the axial symmetry of both the beam and the sample, we solve the problem in a cylindrical coordinate system. We use a radially polarized beam here to ensure that the azimuthal electric component will vanish (i.e., $E_{\varphi}(r, z) = 0$).[39] Using the vectorial angular spectrum method, the electric field distribution can be written as[40]

$$E_r(r,z) = HT^1\left[HT^1[T(r)E(r,0)]\exp\left(i2\pi z\sqrt{\lambda^{-2}-f^2}\right)\right], \quad (1)$$

$$E_z(r,z) = HT^0\left[\frac{if}{\sqrt{\lambda^{-2}-f^2}}HT^1[T(r)E(r,0)]\exp\left(i2\pi z\sqrt{\lambda^{-2}-f^2}\right)\right]. \quad (2)$$

Here, HT^0 and HT^1 represent the zeroth- and the first-order Hankel transformations, respectively. $T(r)$ is the transmission function of the sample, and $E(r, 0)$ is decided by the incident electric field at $z = 0$. λ is the SH wavelength and f is the spatial frequency. Considering that the positive and negative domains in a PPLN sample introduce 0 and π phase modulations, respectively, in the generated SH waves, one can easily obtain $T(r)$ for a given sample structure. Then, one can use Eqs. (1) and (2) to design an appropriate domain structure that can generate a sub-diffraction SH optical needle with a long DOF.

To obtain the optimal distribution for the domains, a genetic algorithm (GA) is used, and the SH light is set to be a 450 nm radially polarized beam. The target is to achieve an SH needle as long as possible while keeping its sub-diffraction property. In our algorithm, the population, crossover probability, and mutation probability are set to be 150, 0.8, and 0.8, respectively. The evaluate fitness and constraint functions are all vectorized to improve the efficiency of numerical calculations. The longitudinal polarization component is dominant in the generated SH optical needle.[11,39,40] The optimal structure calculated using the GA is shown in Fig. 1(a). The binary domains are arranged in concentric rings, where the white and black rings represent the positive and negative domains, respectively. The width of these rings (or domains) is about 3 μm, and the duty cycle is ~50%. We design an unpoled area in the central area of the PPLN sample to improve the quality of the SH optical needle.[13,41] We calculate the full width at half maximum (FWHM) and the intensity of the optical needle along the propagation path. As shown in Fig. 1(b), we define the part with an intensity higher than 20% of the peak intensity as the optical needle, which ranges from 12.5 μm to 28.8 μm. The simulated FWHM (blue points) is well beyond $\lambda_{SH}/2$ (red line) throughout the range, which presents a well-defined sub-diffraction SH optical needle.

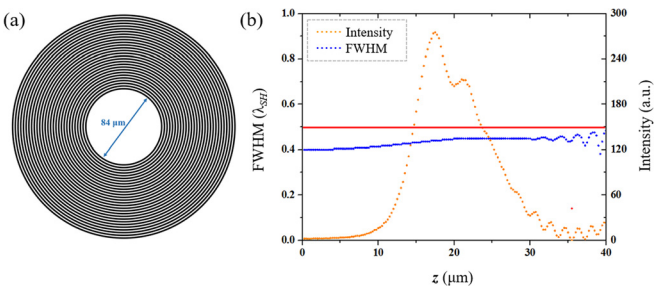

FIG. 1. (a) Pattern of domain structures. The central diameter is 84 μm, the ring width is 3 μm, and the white and black rings represent the positive and the negative domains, respectively. (b) Illumination of the FWHM and the intensity of the optical needle along the propagation path. Blue points: FWHM; orange points: intensity; red line: $\lambda_{SH}/2$.

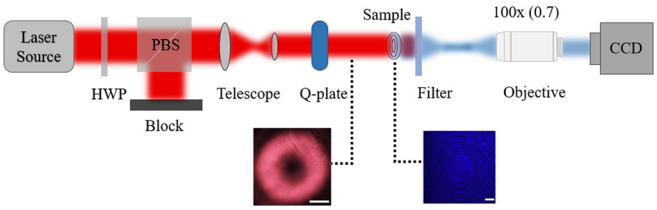

FIG. 2. Experimental setup. The fundamental wavelength is 900 nm. The insets show the cross section of the radially polarized incident light (left, the scale bar is 100 μm) and the SH image of the sample (right, the scale bar is 20 μm). HWP: half-wave plate; PBS: polarizing beam splitter; CCD: charge coupled device. Note that the objective and the CCD are mounted on a microscope.

In the experiment, the $LiNbO_3$ crystal with its ring-shaped domain structures is fabricated using photolithography and electrical poling process. First, a 40-μm-thick z-cut $LiNbO_3$ slice is cleaned and spin-coated with photoresist. We then transfer the domain structure pattern [Fig. 1(a)] to the prepared $LiNbO_3$ slice via maskless photolithography. Cr electrodes with the designed ring structures are affixed to the $+z$ surface of the $LiNbO_3$ slice after a series of coating and lift-off processes. Finally, electrical poling is performed on the $LiNbO_3$ slice to achieve the designed ferroelectric domain structures. During poling, the $-z$ surface of the sample is placed on an ITO glass substrate, which acts as a uniform electrode. The change in the signs of the second-order nonlinear susceptibility of the sample produced by poling results in a π-phase difference for the relevant SH waves, while the fundamental wave (FW) propagates along the z-axis without changing.[42]

The experimental setup is as shown in Fig. 2. A horizontally polarized FW from a Ti: sapphire femtosecond laser (pulse width: 75 fs; repetition rate: 80 MHz) is passed through a half-wave plate

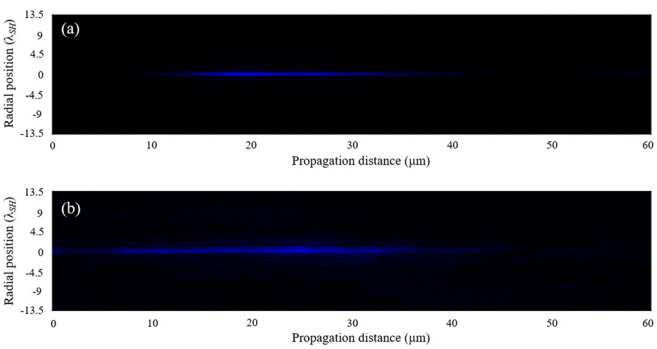

FIG. 3. Propagation carpet of the SH optical needle: (a) theory and (b) experiment.

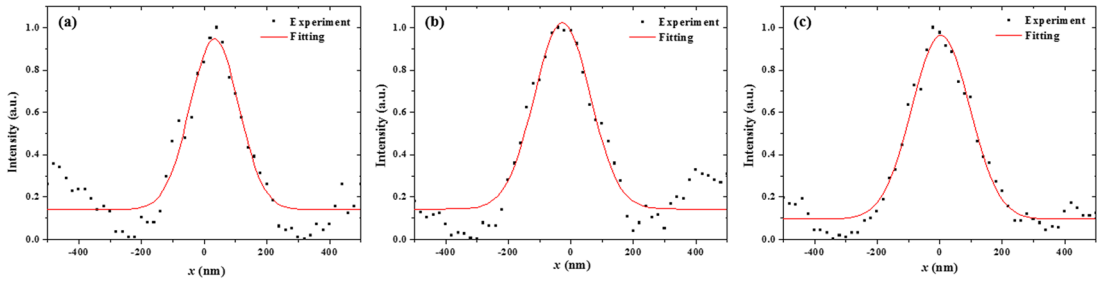

FIG. 4. Normalized optical needle intensity profiles at z = 9 μm (a), 23 μm (b), and 33 μm (c).

(HWP) and a polarizing beam splitter (PBS) to control its power at ~300 mW. The fundamental light is set at a wavelength of λ_{FW} = 900 nm. A telescope system that consists of two convex lenses is applied to collimate the incident beam and reduce its size to 300 μm to match the sample size. The radially polarized beam is generated by using a Q-plate.[43,44] After the FW is filtered out, only the SH wave generated at a wavelength of 450 nm is collected via a 100× objective lens and recorded using a charge coupled device (CCD). The exposure time of the CCD is 1 ms.

We record the propagation carpet of the SH optical needle experimentally. First, the sample is located accurately on the focal plane of the objective lens ($z = 0$). We then record the cross sections (x-y) at different positions along the propagation direction z by varying the distance between the sample and the objective. Therefore, a sequence of SH intensity patterns within propagation distances ranging from 0 to 60 μm is recorded by using a step interval of 0.5 μm. The theoretical and experimental propagation carpets are shown in Figs. 3(a) and 3(b), respectively. In theory, the bright SH optical needle exists in a range from $z = 12.5$ μm to $z = 28.8$ μm, and its DOF is $36\lambda_{SH} \pm 2\lambda_{SH}$. The average spot size of the needle is approximately $0.43\lambda_{SH}$ (193.5 nm), which is well beyond the diffraction limit. In the experiment, the SH optical needle is observed from $z = 8$ μm to $z = 33$ μm. To enable further study of the sub-diffraction characteristics of the optical needle in the experiment, we investigate three cross sections at $z = 9$ μm, 23 μm, and 33 μm. The FWHM is obtained by curve fitting, and the data are normalized. As shown in Figs. 4(a)–4(c), the FWHM values are $0.41\lambda_{SH}$ (185 nm), $0.47\lambda_{SH}$ (212 nm), and $0.48\lambda_{SH}$ (216 nm), respectively, and all these values are beyond the diffraction limit and reflect the good properties of the optical needle. In general, the experimental results agree well with the theoretical results. The average FWHM of $0.45\lambda_{SH}$ (203 nm) in the experiment is a little higher than that obtained from the theory, which could be caused by the defects and non-ideal duty cycle in the PPLN sample and the inaccurate control of the beam waist. Interestingly, the experimental optical needle is longer than the theoretical needle, which may result from the higher FWHM in the experiment.

In conclusion, we have demonstrated an SH optical needle with a sub-diffraction FWHM and an ultra-long DOF in a PPLN crystal pumped by a femtosecond radially polarized light. Using the vectorial angular spectrum method, the electrical field distribution behind the sample is calculated. Note that the opposing domain structures in PPLN slices introduce a π phase difference for the SH wave. In our experimental demonstration, this binary nonlinear phase modulation device can produce an optical needle with a sub-diffracted beam size of $0.45\lambda_{SH}$ and an ultra-long DOF of $55\lambda_{SH}$. An SH optical needle in the visible band is realized through nonlinear frequency doubling, which can further improve the resolution in imaging. The ultra-long DOF makes it possible to observe the object with a certain thickness, which would be difficult when using conventional imaging systems. By improving the PPLN sample quality and optimizing the pump beam profile, the performance of the SH optical needle, such as the longitudinal intensity distribution, could be further improved for practical applications in optical microscopy.[45–47] Our results open the door for a variety of applications of the optical needle in super-resolution imaging and large depth of field imaging.

This work was supported by the National Key R&D Program of China (Nos. 2017YFA0303703 and 2016YFA0302500), the National Natural Science Foundation of China (NSFC) (Nos. 91950206, 11874213, and 91636106), the National Science Foundation of Guangdong Province (No. 2019A1515011401), and Fundamental Research Funds for the Central Universities (No. 1480605201).

REFERENCES

[1]E. Abbe, Arch. Mikrosk. Anat. Entwicklungsmech. **9**(1), 413 (1873).
[2]S. W. Hell and J. Wichmann, Opt. Lett. **19**(11), 780 (1994).
[3]K. I. Willig, S. O. Rizzoli, V. Westphal, R. Jahn, and S. W. Hell, Nature **440**(7086), 935 (2006).
[4]E. Betzig, G. H. Patterson, R. Sougrat, O. W. Lindwasser, S. Olenych, J. S. Bonifacino, M. W. Davidson, J. Lippincott-Schwartz, and H. F. Hess, Science **313**(5793), 1642 (2006).
[5]M. J. Rust, M. Bates, and X. Zhuang, Nat. Methods **3**, 793 (2006).
[6]M. G. L. Gustafsson, J. Microsc. **198**(2), 82 (2000).
[7]M. G. L. Gustafsson, Proc. Natl. Acad. Sci. U. S. A. **102**(37), 13081 (2005).
[8]R. M. Dickson, A. B. Cubitt, R. Y. Tsien, and W. E. Moerner, Nature **388**(6640), 355 (1997).
[9]W. E. Moerner and L. Kador, Phys. Rev. Lett. **62**(21), 2535 (1989).
[10]T. A. Planchon, L. Gao, D. E. Milkie, M. W. Davidson, J. A. Galbraith, C. G. Galbraith, and E. Betzig, Nat. Methods **8**(5), 417 (2011).
[11]H. Wang, L. Shi, B. Lukyanchuk, C. Sheppard, and C. T. Chong, Nat. Photonics **2**(8), 501 (2008).
[12]S. Wang, X. Li, J. Zhou, and M. Gu, Opt. Lett. **39**(17), 5022 (2014).
[13]E. T. F. Rogers, S. Savo, J. Lindberg, T. Roy, M. R. Dennis, and N. I. Zheludev, Appl. Phys. Lett. **102**(3), 031108 (2013).
[14]J. Diao, W. Yuan, Y. Yu, Y. Zhu, and Y. Wu, Opt. Express **24**(3), 1924 (2016).
[15]K. Hu, Z. Chen, and J. Pu, Opt. Lett. **37**(16), 3303 (2012).
[16]G. H. Yuan, E. T. Rogers, and N. I. Zheludev, Light: Sci. Appl. **6**(9), e17036 (2017).
[17]Y. Zhu, D. Wei, Z. Kuang, Q. Wang, Y. Wang, X. Huang, Y. Zhang, and M. Xiao, Sci. Rep. **8**(1), 11591 (2018).

[18]T. Liu, S. Yang, and Z. Jiang, Opt. Express **24**(15), 16297 (2016).
[19]X. Fang, G. Yang, D. Wei, D. Wei, R. Ni, W. Ji, Y. Zhang, X. Hu, W. Hu, and Y. Q. Lu, Opt. Lett. **41**(6), 1169 (2016).
[20]D. Wei, Y. Zhu, W. Zhong, G. Cui, H. Wang, Y. He, Y. Zhang, Y. Lu, and M. Xiao, Appl. Phys. Lett. **110**(26), 261104 (2017).
[21]Y. Wang, D. Wei, Y. Zhu, X. Huang, X. Fang, W. Zhong, Q. Wang, Y. Zhang, and M. Xiao, Appl. Phys. Lett. **109**(8), 081105 (2016).
[22]S. P. Hoffmann, M. Albert, N. Weber, D. Sievers, J. Forstner, T. Zentgraf, and C. Meier, ACS Photonics **5**(5), 1933 (2018).
[23]M. Scalora, J. P. Dowling, C. M. Bowden, and M. J. Bloemer, Phys. Rev. Lett. **73**(10), 1368 (1994).
[24]A. M. Branczyk, A. Fedrizzi, T. M. Stace, T. C. Ralph, and A. G. White, Opt. Express **19**(1), 55 (2011).
[25]S. T. Le, V. Aref, and H. Buelow, Nat. Photonics **11**(9), 570 (2017).
[26]G. Moille, S. Combrié, and A. D. Rossi, Phys. Rev. A **94**(2), 023814 (2016).
[27]L. Wang, Y. Gao, M. Wan, X. Wang, X. Feng, B. Guan, and J. Yao, Opt. Express **24**(26), 29705 (2016).
[28]T. Tyborski, S. Kalusniak, S. Sadofev, F. Henneberger, M. Woerner, and T. Elsaesser, Phys. Rev. Lett. **115**(14), 147401 (2015).
[29]M. Virkki, O. Tuominen, A. Forni, M. Saccone, P. Metrangolo, G. Resnati, M. Kauranen, and A. Priimagi, J. Mater. Chem. C **3**(13), 3003 (2015).
[30]D. Wei, W. Chaowei, W. Huijun, H. Xiaopeng, W. Dan, F. Xinyuan, Z. Yong, W. Dong, H. Yanlei, and L. Jiawen, Nat. Photonics **12**(10), 596 (2018).
[31]T. Xu, K. Switkowski, X. Chen, S. Liu, K. Koynov, H. Yu, H. Zhang, J. Wang, Y. Sheng, and W. Krolikowski, Nat. Photonics **12**(10), 591 (2018).
[32]C. Wang, Z. Li, M. H. Kim, X. Xiong, X. F. Ren, G. C. Guo, N. Yu, and M. Loncar, Nat. Commun. **8**(1), 2098 (2017).
[33]D. Wei, C. Wang, X. Xu, H. Wang, Y. Hu, P. Chen, J. Li, Y. Zhu, C. Xin, X. P. Hu, Y. Zhang, D. Wu, J. Chu, S. N. Zhu, and M. Xiao, Nat. Commun. **10**(1), 4193 (2019).
[34]T. Ellenbogen, N. Voloch-Bloch, A. Ganany-Padowicz, and A. Arie, Nat. Photonics **3**(7), 395–398 (2009).
[35]D. Kasimov, A. Arie, E. Winebrand, G. Rosenman, A. Bruner, P. Shaier, and D. Eger, Opt. Express **14**(20), 9371 (2006).
[36]S. Saltiel, W. Krolikowski, D. Neshev, and Y. S. Kivshar, Opt. Express **15**(7), 4132 (2007).
[37]S. M. Saltiel, D. N. Neshev, R. Fischer, W. Krolikowski, A. Arie, and Y. S. Kivshar, Jpn. J. Appl. Phys., Part 1 **47**(8), 6777 (2008).
[38]J. Wang, W. Chen, and Q. Zhan, Opt. Express **18**(21), 21965 (2010).
[39]R. Dorn, S. Quabis, and G. Leuchs, Phys. Rev. Lett. **91**(23), 233901 (2003).
[40]Z. Chen, Y. Zhang, and M. Xiao, J. Opt. Soc. Am. B **32**(8), 1731 (2015).
[41]T. Roy, E. T. F. Rogers, G. Yuan, and N. I. Zheludev, Appl. Phys. Lett. **104**(23), 231109 (2014).
[42]D. Wei, D. Liu, X. Hu, Y. Zhang, and M. Xiao, Laser Phys. Lett. **11**(9), 095402 (2014).
[43]L. Marrucci, C. Manzo, and D. Paparo, Phys. Rev. Lett. **96**(16), 163905 (2006).
[44]Q. Guo, C. Schlickriede, D. Wang, H. Liu, Y. Xiang, T. Zentgraf, and S. Zhang, Opt. Express **25**(13), 14300 (2017).
[45]L. Turquet, X. Zang, J.-P. Kakko, H. Lipsanen, G. Bautista, and M. Kauranen, Opt. Express **26**(21), 27572 (2018).
[46]N. Vuillemin, P. Mahou, D. Débarre, T. Gacoin, P.-L. Tharaux, M.-C. Schanne-Klein, W. Supatto, and E. Beaurepaire, Sci. Rep. **6**(1), 29863 (2016).
[47]L. Turquet, J. P. Kakko, L. Karvonen, H. Jiang, E. Kauppinen, H. Lipsanen, M. Kauranen, and G. Bautista, J. Opt. **19**(8), 084011 (2017).